Received on Sep 2020

Journal of Soft Computing and Engineering Applications

https://srkpublication.org/

Detection and ClassificationCOVID-19 based on Mask-R-CNN Classifier with Anopheles Search Optimization Algorithm

Arun Kumar T [*], S. Selva raju [2]

[1]*Assistant Professor, Department of Electronics and Communication Engineering, Hindustan college of Engineering & Technology, Coimbatore, Tamil Nadu 641050, India*

[2]*Department of Electronics and Communication Engineering, Arunai Engineering College, Tamil Nadu, India*

[*]Corresponding author email: arunkumar15555@gmail.com

Abstract: The corona virus causes many respiratory diseases and RNA kind viruses can infect both humans and animal. Artificial intelligence models are useful for successful analysis on biomedical field. The corona virus is noticed by the subtype of artificial intelligence in deep learning procedure. Dataset has three classes, that is: corona virus, pneumonia, and normal X-ray imaging. The original data set was recreated with the Fuzzy Gray Level Difference Histogram Equalization technique, which is aimed for color enhancement with eliminate noise on original images. Every fuzzy color is integrated with original imagery to create the best quality image data for the novel data set. The stacked database compressor is trained to Squeeze Net deep convolutional neural network model and the feature packages obtained via the samples are processed by Anopheles search method. Subsequently, the efficient characteristics were combined and classified by Butter Fly algorithm based parameter optimized Mask R-CNN. Here, it is clear that the proposed strategy may contribute effectively to COVID-19 diagnosis.

Keywords: COVID-19, normal, pneumonia, fuzzy color techniques, stacking techniques, Anopheles search algorithm, deep convolutional neural network, *Mask-R-CNN Classifier.*

1. INTRODUCTION

Wuhan's novel Corona Virus (2019-nCoV) is presently causing concern within medical profession because the virus is spreading throughout the world. On the end of December 2019, the count of cases imported from China to other countries is increasing; therefore the epidemiological picture is varying day by day [1]. Complete cases of the single virus are emerging worldwide; the entire eye has focused on the market of seafood at Wuhan, China, from outbreak source [2].

Currently, COVID-19 is the main explanation of death internationally, with main deaths found inUS, Spain, Italy, China, the United Kingdom, and Iran. There are numerous kinds of corona viruses, and such viruses are usually found on animals. COVID-19 is exposed on humans, bats, pigs; Cat, dog, rodent and chicken. COVID-19 symptoms comprise pharyngitis, headache, fever, so on [3]. COVID-19 is transferred from one person to other through physically contact. Lately, artificial intelligence (AI) has been broadly

utilized to accelerate biomedical research. Through in-depth learning strategies, AI is employed at numerous applications, like image detection, data classification, and segmentation [4]. The virus can spread to the lungs and cause pneumonia in people with COVID-19. The first case was find out on 1st Dec, 2019 and no contact with the seafood market is reported. No epidemiological link is initiated among primary patient and subsequent cases. In total, its data show 13 of 41 cases had no relation toward market [5]. This is a giant number, 13, without any connection, says Daniel Lucy, an epidemiologist in Georgetown University [6]. Therefore, previous reports by Chinese health officials said that the primary health patient began to show symptoms on 8th Dec, 2019, and that those reports were easily related to the seafood market that closed on 1st Jan [7].

Between the measures taken to stop the spread of the virus, it may be an important issue to examine the genetic sequence of COVID-19 by monitoring the progression of the COVID-19 infection to see if it spreads internationally. [8]. At present, these efforts depend upon sequencing the COVID-19 genome in patient samples or on virus isolated from patient samples within cell culture [9]. As expected, infectious respiratory viruses are spread primarily by contact with respiratory droplets (> 5 µm). Though, there is growing evidence that COVID-19 spreads the virus well into particles (<5 µm) in aerosols formed while coughs, sneezes, breathes, speaks of infected patient [10]. Thus, controlling the spread of virus becomes the foremost challenging task, so it's necessary to detect the disease with high accuracy for rapid enactment.

The main contributions are following,

- For proposing strategy to divide chest imaging of COVID-19 infection as usual chest images and pneumonia.
- An original dataset is versed inpre-image processing ways. Initially, dataset is reproduced through the Fuzzy Gray Level Difference Histogram Equalization technique, which is aimed for color enhancement and to get rid of noise within original images.
- Secondly, the initial dataset Focus Stacking system, every fuzzy color image is combined to original images, as well as replacement dataset is produced to form a better-quality image data.
- In the following step, stacked dataset is qualified by Squeeze Net deep convolutional Neural Network model and therefore the feature packages acquired via the models are processed by Anopheles Search Algorithm.
- Subsequently, efficient features were combined and categorized by Butter Fly Algorithm based parameter optimized Mask R-CNN Classifier.
- The proposed approach is implemented in MATLAB and it's obvious that the model may professionally give to the detection of COVID-19 disease.

Remaining manuscript is mentioned as below, in section 2 talks about the literature assess, and Section 3 describes the proposed method. Section 4talks about the structure of dataset, deep convolutional neural network models, and Anopheles search algorithm.Experimental investigation is talk about on Section 5. Section 6 presents the conclusion of this manuscript

2. LITERATURE REVIEW

Among the recent research works associated with COVID-19, a number of the research works are reviewed here.

In Jelodar et al. in (2020) [11] have utilized the automated removal of COVID-19 - consideration as social networks and language process scheme supported by topic modeling to discover numerous problems associated with COVID-19 as public opinion. In addition, they explore how LSTM can use a continuous neural network for sensory classification from COVID-19 concepts. Additionally, the experiments showed which the sample came with an accuracy of 81.15%, which was the next precision of many identified machine learning (ML) methods of COVID-19.

Rajaraman et al. in (2020) [12] have demonstrated the use of repetitive pruned sets of deep learning methods to identify lung expression of COVID-19 with chest radiographs. The disease was caused using new serious respiratory symptoms corona virus 2 called the new corona virus (2019-nCoV). A wide variety of reconstructed image net models were trained with assessed in level of patient generally obtainable CXR groups for discovering representations of modification-specific features. Learned knowledge was well-designed for enhancing performance and generalization within associated categorizing CXRs task as usual, viewing bacterial pneumonia or corona virus abnormality. The most effective performance modes were pruned again and again for reducing the problem and enhance memory effectiveness.

Wang et al. in (2020) [13] have introduced a completely unique noise-resistant framework to discover noise labels for the task of segmentation. They initially announce a loss of dice robust to noise, which was loss of dice generalization for separation and loss of mean absolute error for strength next to noise; they establish COVID-19 pneumonia lesions segmentation network (COPLE-Net) to best serve lesions through diverse scales and manifestation. The experimental outcomes demonstrated were: (1) noise-resistant loss of dice surpasses existing noise-resistant loss functionality (2) COPLE-Net reaches greater execution to next-generation image segmentation networks (3) adaptive Self-ensemble framework considerably surpasses a routine training procedure and outperforms other noise-resistant training strategies within the noisy label learning scenario of COVID-19 pneumonia injury segmentation.

Li et al. in (2020) [14] have given an answer for combating the virus during computing (AI). Few deep learning (DL) process were explained to be successful in the objective, together with generative adversarial networks, extreme ML, long / short term memory. It outlines an integrated bio-communication strategy within different features of data, as a series of structured and unstructured data sources were combined for creating user-friendly sites for clinicians and researchers. The most benefit of AI-based sites was accelerating the COVID-19 diagnosis and treatment. The most current related medical publications and information were researched through the aim of selecting network inputs and objectives which would make easy the achievement of a dependable artificial neural network-based tool for COVID-19 related challenges.

Abdel-Basset et al. in (2020) [15] have aimed to rapidly remove as chest X-ray imagery the tiny equal areas have the recognizing characteristics of COVID-19. Here, presents a hybrid detection method of COVID-19 supported by improved marine predator algorithm (IMPA) for X-ray image segmentation. RDR works to find the particles that were not locate superior solutions in a successive number of repetitions, and thus move those particles towards the most effective solutions up to now. IMPA performance was verified through entry levels among 10 and 100 in 9 chest X-ray imageries compared to five algorithms: Equilibrium Optimizer, whale optimization, sine cosine, Harris-Hawks, Slap Swarm. The new outcomes show the hybrid method surpasses entire methods for the variety of measurements. Additionally, the efficiency of the method was integrated at entire threshold levels within Structured Unity Index Metric including Universal Quality Index Metrics.

3. PROPOSED METHOD

The proposed strategy aims to make the chest images classification with data sets types. This can be a method of separating the COVID-19 chest images of viral infections as usualbreast images and pneumonia.

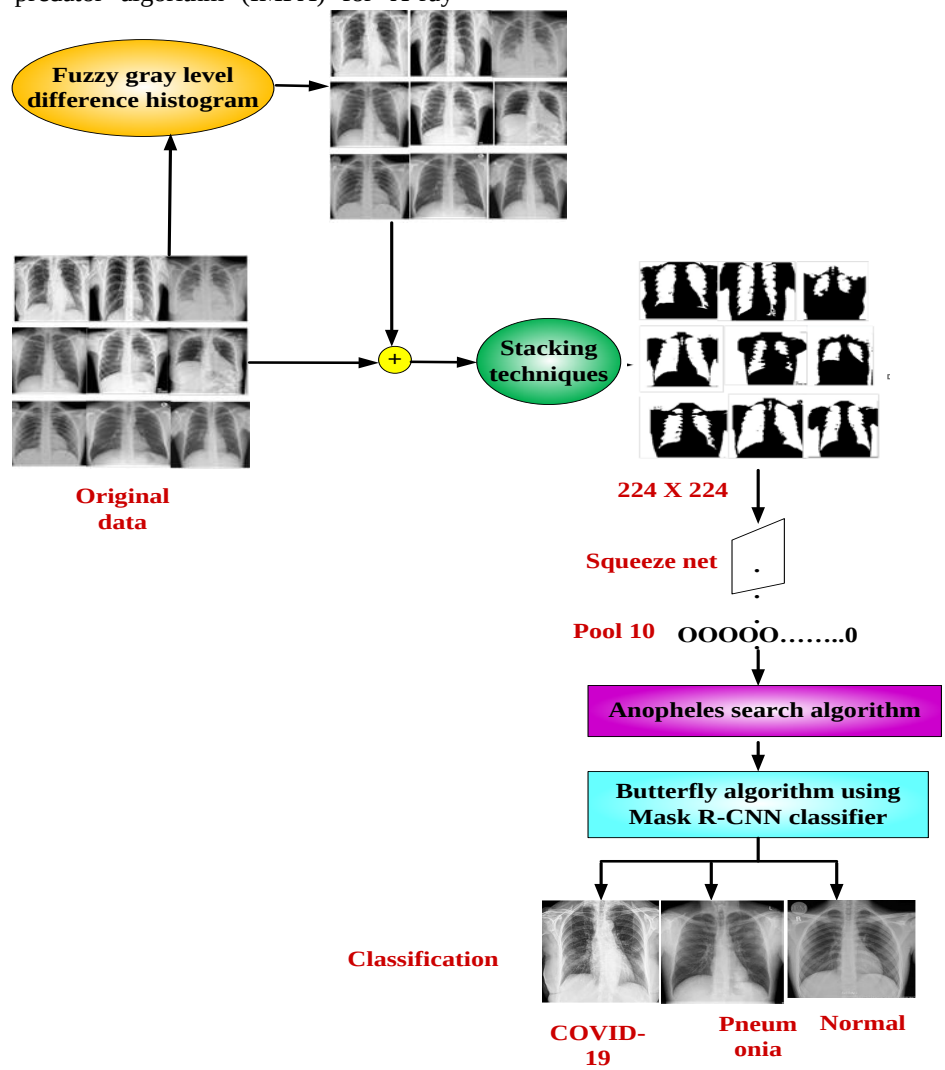

Figure 1: Overall proposed methods

This initial data set is seen in the previous image dispensation modes.Within the initiative, inventive database was recreated using fuzzy gray level difference equalization technique, which aims to color enhancement and eliminate noise on original images.In the next phase, an innovative data set was produced with initial data set for fuzzy stacking system, every fuzzy color image combined within the inventive images for creating the better image quality. Deep convolutional neural network models were employed; therefore the stacked data set was trained by Squeeze Net deep convolutional neural network models. Feature sets are obtained through the models used in the Anopheles search algorithm. Combining the efficient characteristics, the butterfly system created successful outcomes on Mask R-CNN classifier in the classification process.

4. MATERIALS AND METHODS

4.1 Dataset

Here, the three classes of data sets that is publicly available (i) normal, (ii) pneumonia (iii) COVID-19. The initial database of COVID-19 is shared in GitHub website by Joseph Paul Cohen (Montreal University). In this database, the image sets include MERS, SARS, COVID-19, so on [16].

The second COVID-19 database has pictures produced through the team of investigations from the University of Qatar, physicians from Bangladesh, collaborators from Pakistan as well as Malaysia. [17]. The 2 databases of COVID-19 imagery were shared, then 295 images were produced in one innovative dataset [18]. This dataset was significant during this study for verifying COVID-19 chest images by in-depth convolutional neural network model. The second data set has chest images of normal and pneumonia[19].

There are three classes in combined data set. Here, collect the total 295 imagery at COVID-19 group. Normal as well as pneumonia X-ray imagery class of 65 and 98. Figure 1 demonstrates sample image of dataset.

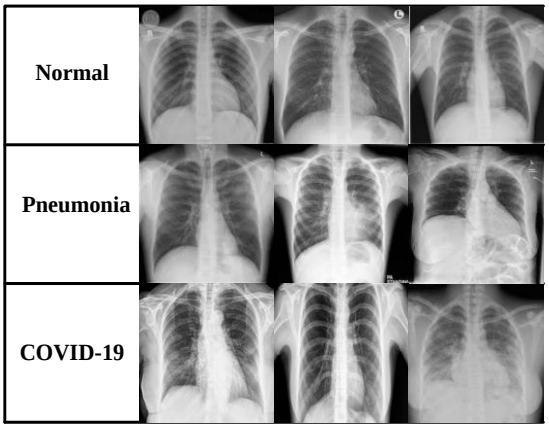

Figure 2: Sample images employed on experimental analysis

4.2 Pre-processing

The preprocessing is the beginning process. The preprocessing system is employed to separate redundant content like noise, lights, and background on provided chest X-ray image. The pre-processing step is to standardize the input and the image size previous to the feature computation. The dataset is renovated by Fuzzy and stacking procedure. To train the data sets by Squeeze Net's deep convolutional neural network models and categorize the models using BF-RF process.

4.2.1 Fuzzy gray level (GL) difference histogram equalization

GL differences are then blurred to cope with the uncertainties present under input image. A fuzzy gray level clipping range is calculated for controlling negligible contrast development [20].

Fuzzy GL difference histogram balancing techniques are featured to improve the contrast in the MR clinical image and not to lose their naturalness. [21] In this case, fuzzy GL is initially computed for eliminating uncertainties under the histogram image, and then followed using clipping process to manage the extreme expansion rate.
The size of input image is m x n,

$$I = \{I(p,q) \mid 0 \le p \le m-1, 0 \le q \le n-1\}$$

The pixel intensity of an input image placed at (a, b) is denoted from I (a, b) =k_s.
here, $s \in \{0,1,\ldots\ldots L-1\}$ where L implies count of intensity levels.

In the following BSP is calculated at R region through L x L dimension wherever the L = 5. The BSP operate from description of the spatial structure, and it is essential to handle noise, intensity inhomogeneity and lighting variations on input image. The entire pattern of comparison go to the R region connected to parameter T_r = 0.3. This parameter simply deals shadows on input image.
BSP P (i_n, i_c) defined the ratio among intensity of central pixels gray level value i_c and neighborhood intensity pixels i_n is given by,

$$P(i_n, i_c) = \begin{cases} 1 & if \mid i_n - i_c \mid \le T_r, i_c \\ 0 & otherwise \end{cases} \quad (2)$$

Gray level difference among intensity of central pixel $i_c$through the linked coordinates (a, b) and the intensity of the neighborhood pixel $i_n$by the linked coordinates (m, n) on region R is computed as

$$X_d(a,b) = \frac{1}{N}[\sum_{m=1}^{L} \sum_{n=1}^{L} P(ic(m,n), in(a,b))] \quad (3)$$

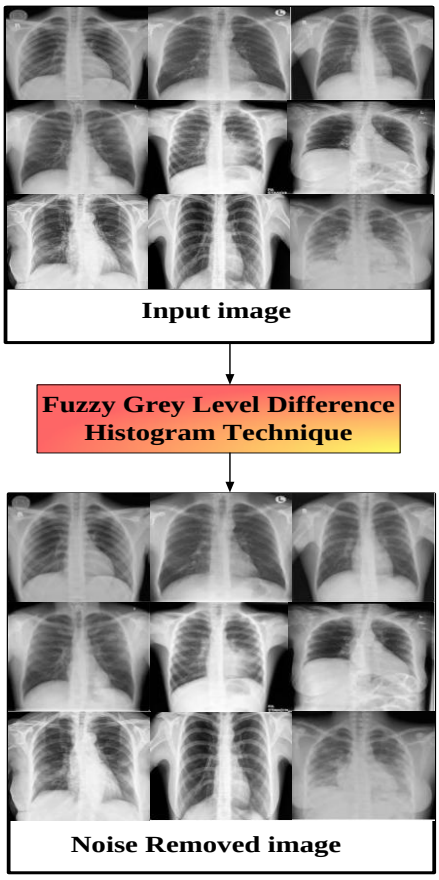

Figure 3: Noise reduction by gray level difference histogram

The Gaussian membership function uses the described gray level differences vaguely,

$$X_{fu}(a,b) = e^{\frac{1}{2}\left(\frac{X_d(a-b)}{\sigma}\right)^2}$$

here, σ implies Gaussian function that may be extended and fitted an exacting weight for assigning the usual interval of grey level difference. This method supports to get the Fuzzy GL differences histogram.

$$h_g(a,b) = \sum_{m=1}^{L} \left(\sum_{n=1}^{L} G_{fu}(a,b)\delta(i(m,n)-g)\right)$$

g = {0; 1; 2; 3; …:255}

here, g implies GL value, I (m, n) indicate pixel intensity value on (m, n) in region R, delta function represents δ.
The noise reduction by fuzzy gray level difference techniques in COVID -19, pneumonia and normal images are in above figure 3.2.1

4.3 Reconstructing image

4.3.1 Stacking techniques

Image stacking could be a image processing system, which mixes multi-images taken or recreates them in changed focal lengths [22]. This is a common way to enhance the standard of photographs within the dataset. This method aspires to remove noise as the initial image by combining a minimum of two images on same row as well asseparating image.

4.3.1.1 Reconstructing procedure

Let $K_{y,z}(x,F_y,F_z)$ implies marginal Fourier transform of reconstructed target function $\bar{f}(x,y,z)$ regarding variable (y,z) and then target function on range $x=x_n$ may be improved via two-dimensional inverse Fourier transform of $K_{y,z}(x=x_n,F_y,F_z)$ with respect to (F_y,F_z) which is,

$$\bar{f}(x=x_n,y,z) = \int_{F_z}\int_{F_y} K_{y,z}(x=x_n,F_y,F_z)\times\exp(jF_y y + jF_z z)dF_Y dF_z \quad (6)$$

where the constant amplitude factor in the Fourier integral is deserted. Comparing equation (6) find the reconstruction of $K_{y,z}(x=x_n,F_y,F_z)$ is,

$$K_{y,z}(x=x_n,F_y,F_z) = \int_{F_w} S(F_w,F_u,F_v)\times S^*_{x_n}(F_w,F_u,F_v)dF_w \quad (7)$$

where,

$$\begin{aligned} F_y &= F_u \\ F_z &= F_v \end{aligned} \quad (8)$$

Basically, the beyond one-dimensional integral may be implemented by adding the obtainable discrete values F_w and Fourier transform digital implementation or their inverse. Thus, the target function is expressed according to discrete form of reconstruction at $(x=x_n,y,z)$

$$\bar{f}(x=x_n,y,z) = IFFT\left\{\sum_{F_w}[FFT_{u,v}\{S(F_w,u,v)\}].S^*_{x_n}(F_w,F_u,F_v)\Delta F_w\right\} \quad (9)$$

During this study, Python and Pillow library is employed to stack system [23]. The initial dataset is stacked on the recreated dataset by Fuzzy system. Satisfactory results of the Fuzzy system will give to the success of stack system. The limit values within the stacking system are set with opacity value, worth of 0.6, contrast value 1.5, brightness value - 80, and combined ratio of 50% is selected. Such

values may still vary in a database. Moreover, initial database is located within the background; also the structured database is located within overlay. The integrated illustration of first database by layering the structure and database is demonstrated in Figure 4.3.1

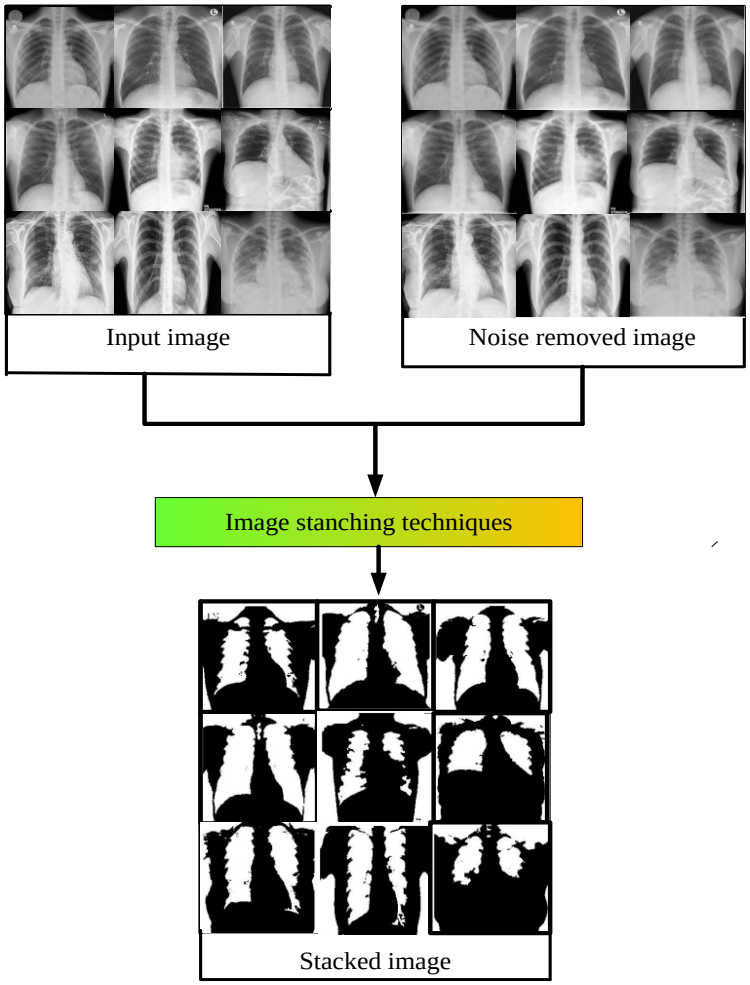

Figure 4: Sub-image samples obtained using stack system.

4.3.2 Fuzzy color techniques

Fuzzy concept is established on the basis of the support of their accuracy, and their subsequent degree is unsure. Fuzzy color mechanisms carry a very significant role on image analysis, as well as outcomes acquired in terms of similarity functions utilized for color separation. Within fuzzy color method, every input image has three input variables (red, green and blue). The input and output values are resolute step by step with training data.

Denoising scheme used is founded on the A statistic explained at below lines. To utilize A instant of B for theireffectivenessin detecting impulses. Assume every pixel x, on RGB format (x (1), x (2), x (3)), n x n window W_x centered at x. let W_x^0 be neighbors pixels of x in W_x, $W_x^0 = W_x - \{x\}$. To compute the B statistics the distance $d_{x,x_i}, x_i \in W_x^0$ are stored in ascending order, obtain a non-negative real set $r_j(x)$ like $r_1(x) \le r_2(x) \le \ldots\ldots\ldots \le r_{n^2-1}(x)$. Then given an integer $0 < \alpha \le n^2 - 1, B_\alpha$ denotes the α rank ordered difference statistic, given by,

$$B_\alpha(x) = \sum_{j=1}^{\alpha} r_j(x) \tag{10}$$

B_α express the global distance amongx and α closest neighbors. This distance is predictableto be superior for the noise fee pixels. The fuzzy metrics M_α is employed for obtaining the distance $d_{x,x_i}, x_i \in W_x^0$, as it proven to particularly sensitive to impulsive noise.

$$M_\alpha(x_i, x_j) = \min_{l=1}^{3} \frac{\min\{x_i(l), x_j(l)\} + P}{\max\{x_i(l), x_j(l)\} + P} \quad (11)$$

The parameter P on equation (11)is set with 1024that has confirmed to be a convenient value of RGB color vectors. The fuzzy distance $d_{x,x_i} = M_\alpha(x, x_i)$ in a decreasing sequence $s_1(x) \geq s_2(x) \geq \ldots\ldots\ldots \geq s_{n^2-1}(x)$ the fuzzy statistic A_α is defined by,

$$A_\alpha(x) = \prod_{j=1}^{\alpha} s_j(x) \quad (12)$$

The positive integer α on equation (12) is a parameter like that $\alpha < n^2 - 1$. An impulse noise pixel will have a minimum value of A_α since it is not probable to equal their neighbors, where impulse free pixels are probable to A_α value nearer to one. $A_\alpha(x)$ That is utilized to recognize pixels that that are obviously impulsive or impulse free.

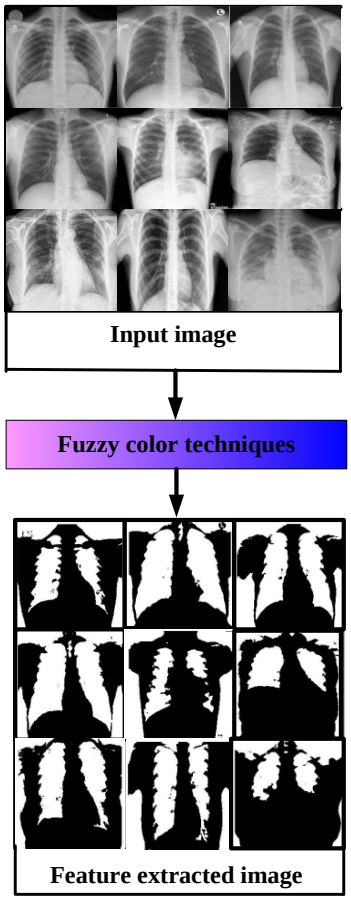

Figure 5: Original dataset obtained using Fuzzy Color system

Every pixel within the image includes a degree of membership in each window, and the degrees of membership are computed depends on gap among window and also pixel. The variation of the image is achieved to degree of affiliation. Fuzzy color system consists of creating the finishing exit entrance [24]. Figure 5 illustrates the information of image structure.

4.4 Squeeze Net deep convolutional Neural Network model

Squeeze Net, a deep learning model with an input size of 224x224 pixels, is made up of convolutional, grouping, ReLU and Fire layers. Squeeze Net has no fully attached layers or dense layers. Though, the layers of fire perform the functions of those equal layers. The best thing about this model is that it makes successful analysis by diminishing the parameter number, thus diminishing the size efficiency of the sample. The Squeeze Net model created more successful outcomes, about 50 times less parameters to AlexNet model, thus decreasing the model value [25]. Though the knowledge regarding the layers is suggested within squeeze net model, the fireplace layers (F2, F3..., F9) look like an innovative layer has two division, specifically the parts of compression and expansion.

4.4.1 Convolutional Layer (CL)

The CL is defined as CNN base layer. It's dependable to pattern decisive characteristics. Here, the input image has been sent via the filter. The consequential values of the filter contain feature map. This layer utilizes few kernels, which slide concluded the pattern for extracting lower with higher level features at the pattern. The kernel has 3x3 or 5x5 shaped matrix to replace along input matrix pattern. Stride factor is the count of phases adjusted for changing over input matrix. The CL output is:

$$x_j^1 = f\left(\sum_{a=1}^{N} W_j^{l-1} * Y_a^{l-1} + b_j^i\right)$$

where, $X_j^{\cdot}$ implies j feature map on layer l, W_j^{l-1} implies j kernels at layer l-1, Y_a^{l-1} implies feature map on layer l-1, b_j^l signifies j feature map bias on layer l, N as count of overall features on layer l-1, (*) signifies vector convolution method.

4.4.2 Pooling Layer (PL)

After the CL, the 2nd layer is defined as pooling layer. The PL is typically utilized to feature maps developed for dropping the count of feature maps with network.

Parameters using consistent mathematical calculation, here, max-pooling with global average pooling are utilized. The max-pooling method chooses only the maximal value depending on matrix size particular in every feature map, as a result the output neurons are reduced. The global average PL is employed prior to fully connected layer (FCL), dropping data toward single measurement. After global average PL, it is linked to FCL. Another intermediate layer is dropout layer. The major aim of this layer is to avoid network over fitting including divergence.

4.4.3 Fully Connected Layer (FCL)

FCL is the final as well as vital layer of convolution NN. The functions of this layer like multiple layer perception. Rectified Linear Unit (ReLU) activation operation is typically utilized in FCL, when Soft ax activation operation is utilized to forecast output imagery at final layer of FCL. Mathematical calculation of these 2 activation operation is:

$$ReLU\ (x) = \begin{cases} 0, & x < 0 \\ x, & x \geq 0 \end{cases} \quad (14)$$

$$\text{Soft max}\ (x_i) = \frac{e^{x_i}}{\sum_{y=1}^{m} e^{x_y}} \quad (15)$$

here x_i indicates input data, m indicates count of classes.

4.5 Anopheles Search Algorithm

The algorithm scans the search space by random search to remove needless information. The performance of the Anopheles optimization algorithm is analyzed by well-known optimization issues. Every solution point, the space could be assumed a child, and its created scent will be in their optimal proportions. Furthermore, the search agents on solution space are considered to be equivalent; the density odor in the natural space may be calculated simply as below:

$$L = a \log (C) + b \quad (16)$$

here, L implies density of odor, C implies weber Fechner chemical concentration coefficient, b refers tracking stable.
In equation (6), if a considered an inverse distance between X_i and point Y_i and C is considered to be optimalpoint on solution space according tothe location $X_i$may be consequent as below,

$$Odor_{X_i Y_i} = \frac{1}{Dist(X_i Y_i)} \times \log(fitness(Y_i)) + b, 0 \leq b \leq 0.5 \quad (17)$$

$$Dist(X_i Y_i) = \sqrt{\sum_{j=1}^{n} (x_j(X_i) - x_j(Y_i))^2} \quad (18)$$

If b=0.5, the odor will enlarge. The closer value of b to their upper one of Anopheles movement maximized. If b=0, then the distance and optimality are employed for computing Anopheles movement.

4.6 Classification method

4.6.1 Butter Fly Algorithm based parameter optimized Mask R-CNNClassifier

The butterfly algorithm can also be used to improve the randomness of large arrays of partially random numbers. This method is used in the classification process for separating characteristics into data classes. Select a location outside of the class characteristics.

The deep convolutional neural network methods use optimization systems and ease learning model tendencies. Mask R-CNN optimization is a way to upgrade the weight parameters on model structure in each repetition. This models offer excellent training for every repetition. Though, Mask R-CNN does not utilize entire input images on the model when upgrading parameters.

4.6.2 Mask R-CNNclassifier

One of the most reliable learning algorithms accessible is Mask R-CNN [26]. It creates an extremely precise classifier for many data sets. Mask R-CNNis a pruned decision trees compilation. When substantial training datasets and a very significant number of input variables, are Mask R-CNNare often used.

The Loss function of Mask=R-CNN is:

$$P_L = P_{class} + P_{box} + P_{mask} \quad (19)$$

where, $P_{class} + P_{box}$ denotes detected similar as in rapid R-CNN, $P_{class} + P_{box}$ is,

(16)

$$P_{class} + P_{box} = \frac{1}{V_{class}} \sum_j P_{class}(L_i, L_i^*) + \frac{1}{V_{box}} \sum_j L_i^* P_1^{smoothe}(r_j - r_j^*) \quad (20)$$

$$P_{Class}\left(\{L_j, L_j^*\}\right) = -L_i^* \log L_j^* - (1 - L_j^*) \log(1 - L_j^*) \quad (21)$$

Then, the P_{mask} is the average binary cross- entropy loss.

$$P_{mask} = -\frac{1}{n^2} \sum_{1 \leq i, j \leq m} \left[X_{ij} \log 0 X_{ji}^H + (1 - X_{ji}) \log(1 - 0 X_{ji}^H) \right] \quad (23)$$

where, F is the fitness function, C_i indicates the number of classified instance and T_s the training samples.

Mask-R-CNN classifier is a successful ensemble learning methods that is demonstrated to the proficient methods in pattern recognition with ML for higher-dimensional classification including skewed issues. Consider a learning set

$$L = ((N_1, M_1).....(N_m, M_m)) \quad (20)$$

Consider m is the vectors, $N \in X$ here X denotes set of numerical or symbolic observations, $M \in Y$ here, Y implies set of class labels. To classification issues, a classifier is defined as mapping $X \to Y$. A newly input vector has been classified through every individual Mask-R-CNN classifier.

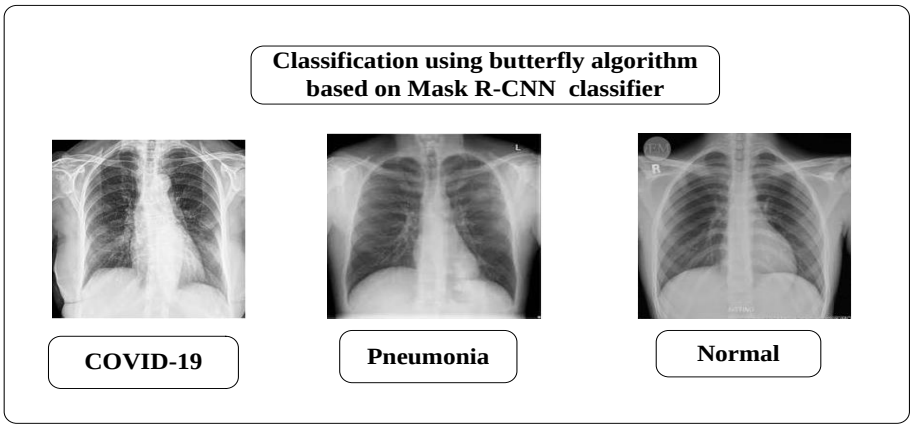

Figure 6: classification model depending on Mask R-CNN classifier

5. EXPERIMENTAL RESULTS AND DISCUSSION

The AS algorithm is compiled in Python, the comprehensive data regarding with source codes, analysis is provided within web link on open ASCII text file. Jupiter Notebook is an interface program employed to compile Python. Through in-depth learning models, MATLAB (2019b) is employed for software classification.

5.1 Performance metrics

5.1.1 Accuracy

The measure of the overall effectiveness of classification system is named as accuracy.

$$\text{Accuracy} = \frac{T_P + T_N}{T_P + T_N + F_P + F_N} \quad (21)$$

5.1.2Specificity

For identifying patterns of a negative class is computed to measure the ability of the classifier.

$$\text{Specificity} = \frac{T_N}{T_N + F_P}$$

5.1.3 Sensitivity

For identifying patterns of a positive class is computed to measure the ability of the classifier.

$$\text{Specificity} = \frac{T_N}{T_N + F_N} \quad (23)$$

5.1.4 F-measure

F-measure creates the use of recall and precision is described as

$$F_{measure} = 2 \times \frac{recall \times precision}{recall + precision} \quad (24)$$

$$Recall = \frac{T_P}{T_P + F_N} \quad (25)$$

$$Precision = \frac{T_P}{T_P + F_P} \quad (26)$$

5.1.5 Mathews correlation coefficient (MCC)

Matthews Correlation Coefficient (MCC) is defined based on true +ve (TP), true –ve (TN), false +ve (FP) and false –ve (FN).

$$MCC = \frac{(T_P \times T_N) - (F_P \times F_N)}{[(T_P + F_N)(T_P + F_P)(T_N + F_P)(T_N + F_N)]^{1/2}} \quad (27)$$

5.1.6 Error rate

The number of all inaccurate forecast separated by a total number in the data set is computed as an error rate.

$$Error_{rate} = \frac{F_P + F_N}{T_P + T_N + F_P + F_N} \quad (28)$$

The PPV and NPV is articulated as

$$PPV = \frac{T_P}{T_P + F_P}$$

$$NPV = \frac{T_N}{T_N + F_N}$$

Although specimens belonging to the selected class are properly recognized via classifier, such specimens are placed in TP codes. Other models belonging to correctly recognized opposite classes are within TN codes within the confusing matrix.

Figure 7 shows the accuracy of the original data can be calculated by COVID -19, normal and pneumonia. The accuracy of proposed squeeze net convolutional neural network provides 96.5 % higher than Mobile net V2 and Res net model in COVID-19 cases. In normal cases the accuracy of the proposed squeeze net convolutional neural network provides 79.47 % higher than Mobile net V2 and Res net model. In pneumonia cases the accuracy of the proposed squeeze net convolutional neural network provides 76.57 % higher than Mobile net V2 and Res net model. By this our proposed squeeze net convolutional neural network provides higher accuracy compared with Mobile net V2 and Res net.

Figure 8 shows the accuracy of the fuzzy techniques can be calculated by COVID -19, normal and pneumonia. The accuracy of proposed squeeze net convolutional neural network provides 98.95% higher than Mobile net V2 and Res net model in COVID-19 cases. In normal cases the accuracy of the proposed squeeze net convolutional neural network provides 98.30 % higher than Mobile net V2 and Res net model. In pneumonia cases the accuracy of the proposed squeeze net convolutional neural network provides 97.60% higher than Mobile net V2 and Res net model in fuzzy techniques our proposed squeeze net convolutional neural network provides higher accuracy compared with Mobile net V2 and Res net.

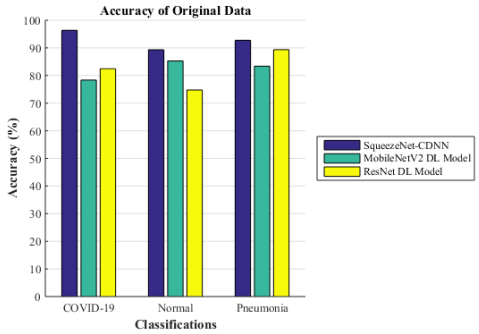

Figure 7: performance analysis of accuracy using original data

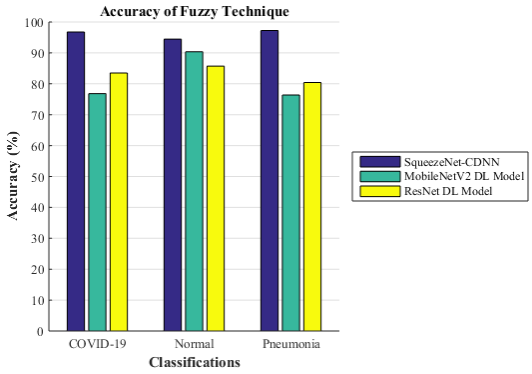

Figure 8: performance analysis of accuracy using fuzzy techniques

Figure 9 shows the accuracy of the stacked techniques can be calculated by COVID -19, normal and pneumonia. The accuracy of proposed squeeze net convolutional neural network provides 99.86% higher than Mobile net V2 and Res net model in COVID-19 cases. In normal cases the accuracy of the proposed squeeze net convolutional neural network provides 99.79% higher than Mobile net V2 and Res net model. In pneumonia cases the accuracy of the proposed squeeze net convolutional neural network provides 98.07% higher than Mobile net V2 and Res net model. In stacked techniques our proposed squeeze net convolutional neural network provides higher accuracy compared with Mobile net V2 and Res net deep learning model.

Figure 10 shows the precision of the squeeze net original data can be calculated by COVID -19, normal and pneumonia. The precision of proposed squeeze net convolutional neural network provides 85.57% higher than Mobile net V2 and Res net model in COVID-19 cases. In normal cases the precision of the Proposed squeeze net convolutional neural network provides 93.13% higher than Mobile net V2 and Res net model. In pneumonia cases the precision of the proposed squeeze net convolutional neural

network provides 97.14% higher than Mobile net V2 and Res net model.in squeeze net original data of our proposed squeeze net convolutional neural network provides higher precision compared with Mobile net V2 and Res net deep learning model.

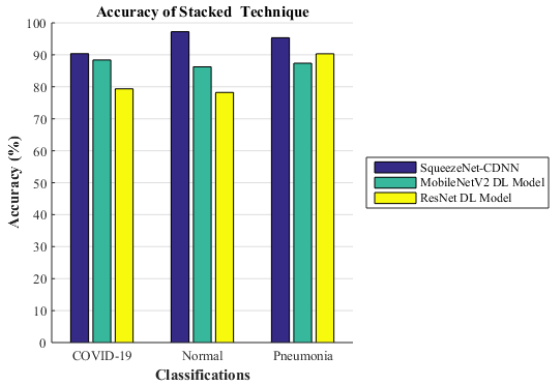

Figure 9: performance analysis of accuracy using stacked techniques

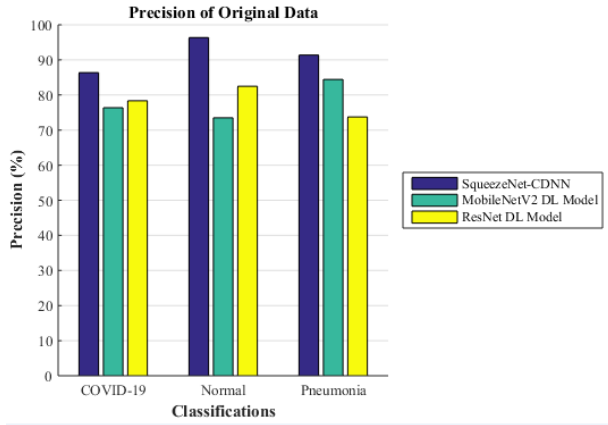

Figure 10: performance analysis of precision using original data

Figure 11 shows the precision of the fuzzy techniques can be calculated by COVID -19, normal and pneumonia. The precision of proposed squeeze net convolutional neural network provides 98.13% higher than Mobile net V2 and Res net model in COVID-19 cases. In normal cases the precision of the proposed squeeze net convolutional neural network provides 85.78% higher than Mobile net V2 and Res net model. In pneumonia cases the precision of the proposed squeeze net convolutional neural network provides 96.19% higher than Mobile net V2 and Res net model. In squeeze net fuzzy techniques of our proposed squeeze net convolutional neural network provides higher precision compared with Mobile net V2 and Res net deep learning model.

Figure 12 shows the precision of the stacked techniques can be calculated by COVID -19, normal and pneumonia. A precision of proposed squeeze net convolutional neural network provides 97.63% higher than Mobile net V2 and Res net model in COVID-19 cases. In normal cases the precision of the proposed squeeze net convolutional neural network provides 91.58% higher than Mobile net V2 and Res net model. In pneumonia cases the precision of the proposed squeeze net convolutional neural network provides 95.29% higher than Mobile net V2 and Res net model.in squeeze net stacked techniques of our proposed squeeze net convolutional neural network provides higher precision compared with Mobile net V2 and Res net deep learning model

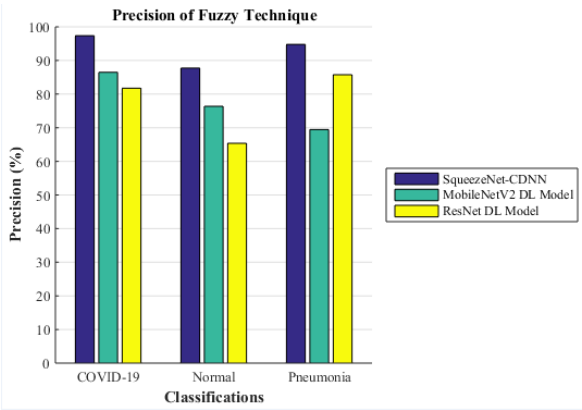

Figure 11: performance analysis of precision using fuzzy techniques

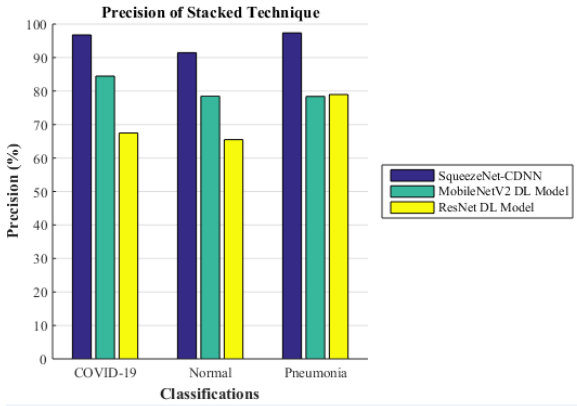

Figure 12: performance analysis of precision using stacked techniques

Figure 13 shows the specificity of the original data can be calculated by COVID -19, normal and pneumonia. A specificity of proposed squeeze net convolutional neural network provides 91.67% higher than Mobile net V2 and Res net model in COVID-19 cases. In normal cases the specificity of the proposed squeeze net convolutional neural network provides 79.58% higher than Mobile net V2 and Res net model. In pneumonia cases the specificity of the proposed squeeze net convolutional neural network provides 88.19% higher than Mobile net V2 and Res net model.in squeeze net original data of our proposed squeeze net convolutional neural network provides higher specificity

compared with Mobile net V2 and Res net deep learning model.

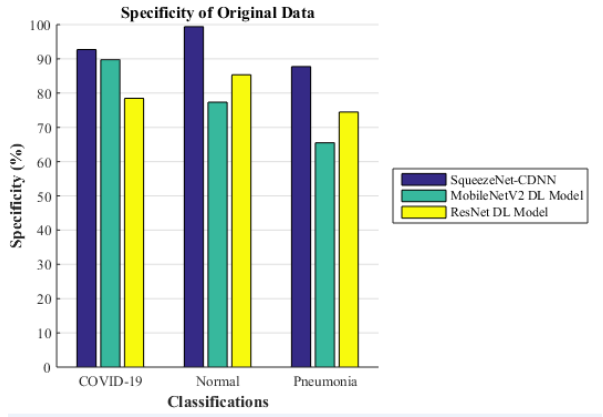

Figure 13: performance analysis of specificity using original data

Figure 14 shows the specificity of the fuzzy techniques can be calculated by COVID -19, normal and pneumonia. A specificity of proposed squeeze net convolutional neural network provides 98.67% higher than Mobile net V2 and Res net model in COVID-19 cases. In normal cases the specificity of the proposed squeeze net convolutional neural network provides 97.58% higher than Mobile net V2 and Res net model. In pneumonia cases the specificity of the proposed squeeze net convolutional neural network provides 94.28% higher than Mobile net V2 and Res net model in fuzzy techniques of our proposed squeeze net convolutional neural network provides higher specificity compared with Mobile net V2 and Res net deep learning model.

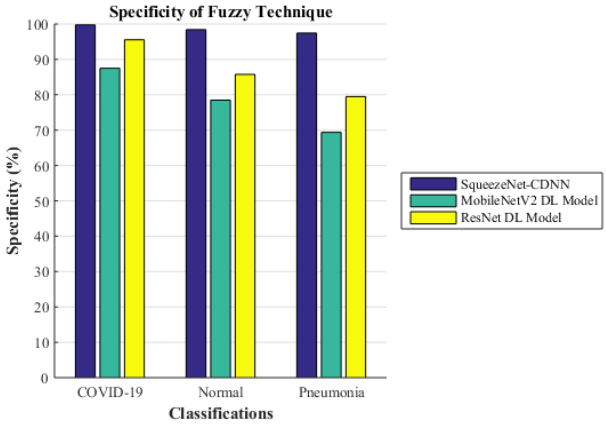

Figure 14: performance analysis of specificity using fuzzy techniques

Figure 15 shows the specificity of the stacked techniques can be calculated by COVID -19, normal and pneumonia. A specificity of proposed squeeze net convolutional neural network provides 97.97% higher than Mobile net V2 and Res net model in COVID-19 cases. In normal cases the specificity of the proposed squeeze net convolutional neural network provides 95.28% higher than Mobile net V2 and Res net model. In pneumonia cases the specificity of the proposed squeeze net convolutional neural network provides 93.28% higher than Mobile net V2 and Res net model.in stacked techniques of our proposed squeeze net convolutional neural network provides higher specificity compared with Mobile net V2 and Res net deep learning model

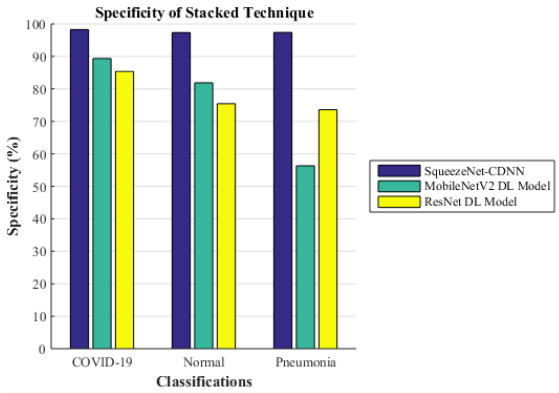

Figure 15: performance analysis of specificity using stacked techniques

Figure 16 shows the sensitivity of the original data can be calculated by COVID -19, normal and pneumonia. A sensitivity of proposed squeeze net convolutional neural network provides 95.91% higher than Mobile net V2 and Res net model in COVID-19 cases. In normal cases the sensitivity of the proposed squeeze net convolutional neural network provides 78.58% higher than Mobile net V2 and Res net model. In pneumonia cases the sensitivity of the proposed squeeze net convolutional neural network provides 81.28% higher than Mobile net V2 and Res net model in original data of our proposed squeeze net convolutional neural network provides higher sensitivity compared with Mobile net V2 and Res net deep learning model.

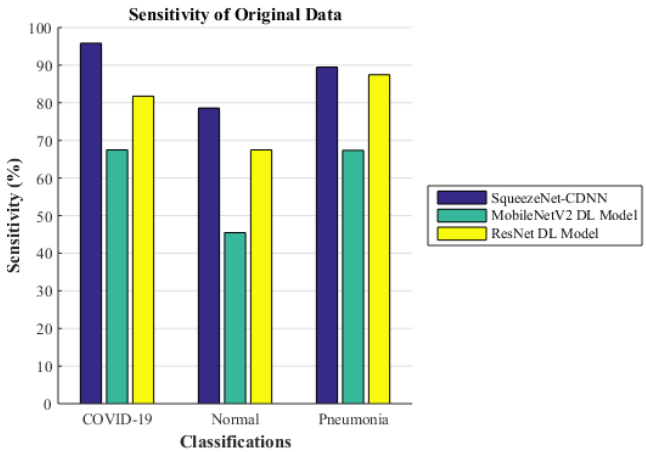

Figure 16: performance analysis of sensitivity using original data

Figure 17 shows the sensitivity of the fuzzy techniques can be calculated by COVID -19, normal and pneumonia. A

sensitivity of proposed squeeze net convolutional neural network provides 93.81% higher than Mobile net V2 and Res net model in COVID-19 cases. In normal cases the sensitivity of the proposed squeeze net convolutional neural network provides 96.18% higher than Mobile net V2 and Res net model. In pneumonia cases the sensitivity of the proposed squeeze net convolutional neural network provides 87.98% higher than Mobile net V2 and Res net model.in fuzzy techniques of our proposed squeeze net convolutional neural network provides higher sensitivity compared with Mobile net V2 and Res net deep learning model

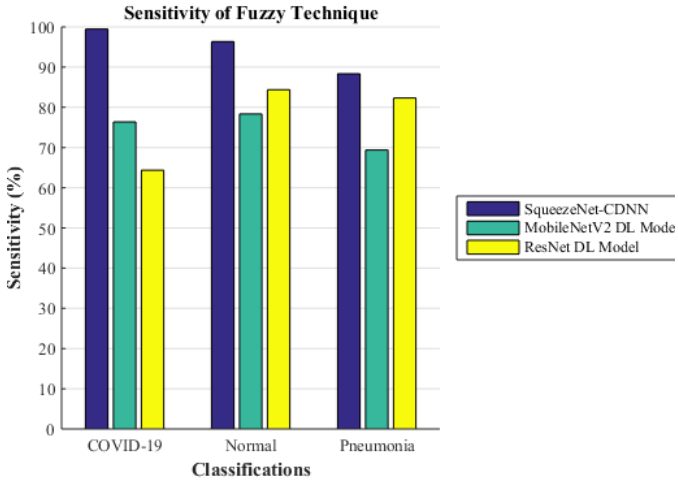

Figure 17: performance analysis of sensitivity using fuzzy techniques

Figure 18 shows the sensitivity of the stack techniques can be calculated by COVID -19, normal and pneumonia. The sensitivity of proposed squeeze net convolutional neural network provides 95.31% higher than Mobile net V2 and Res net model in COVID-19 cases. In normal cases the sensitivity of the proposed squeeze net convolutional neural network provides 91.18% higher than Mobile net V2 and Res net model. In pneumonia cases the sensitivity of the proposed squeeze net convolutional neural network provides 97.58% higher than Mobile net V2 and Res net model.in stacked techniques of our proposed squeeze net convolutional neural network provides higher sensitivity compared with Mobile net V2 and Res net deep learning model

Figure 19 shows the f-measure of the original data can be calculated by COVID -19, normal and pneumonia. The f-measure of proposed squeeze net convolutional neural network provides 97.51% higher than Mobile net V2 and Res net model in COVID-19 cases. In normal cases the f-measure of the proposed squeeze net convolutional neural network provides 73.18% higher than Mobile net V2 model and lowers than and Res net model. In pneumonia cases the f-measure of the proposed squeeze net convolutional neural network provides 81.28% higher than Mobile net V2 and Res net model.in original data of our proposed squeeze net convolutional neural network provides higher f-measure compared with Mobile net V2 and Res net deep learning model

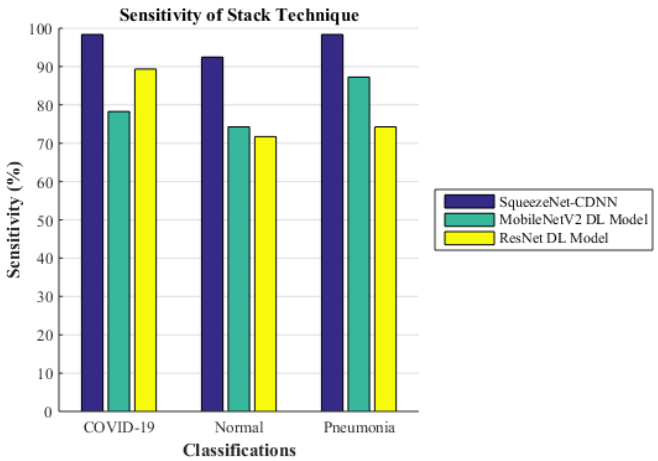

Figure 18: performance analysis of sensitivity using stack techniques

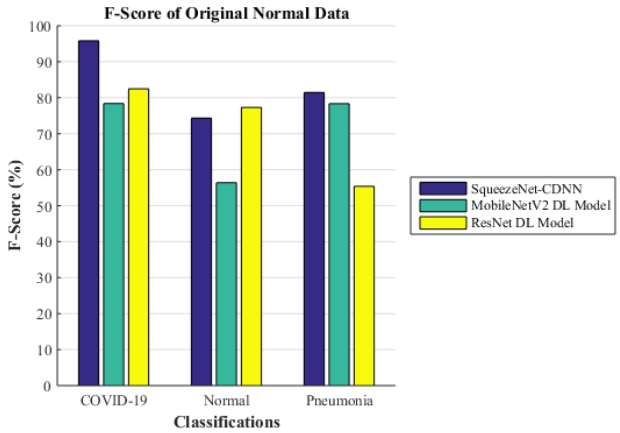

Figure 19: performance analysis of f-score using original data

Figure 20 shows the f-measure of the fuzzy techniques can be calculated by COVID -19, normal and pneumonia. The f-measure of proposed squeeze net convolutional neural network provides 98.31% higher than Mobile net V2 and Res net model in COVID-19 cases. In normal cases the f-measure of the proposed squeeze net convolutional neural network provides 89.18% higher than Mobile net V2 model and Res net model. In pneumonia cases the f-measure of the proposed squeeze net convolutional neural network provides 91.23% higher than Mobile net V2 and Res net model.in fuzzy techniques of our proposed squeeze net convolutional neural network provides higher f-measure compared with Mobile net V2 and Res net deep learning model

Figure 21 shows the f-measure of the stacked techniques can be calculated by COVID -19, normal and pneumonia. The f-measure of proposed squeeze net convolutional neural network provides 94.42% higher than

Mobile net V2 and Res net model in COVID-19 cases. In normal cases the f-measure of the proposed squeeze net convolutional neural network provides 96.38% higher than Mobile net V2 model and Res net model. In pneumonia cases the f-measure of the proposed squeeze net convolutional neural network provides 97.53% higher than Mobile net V2 and Res net model.in stacked techniques of our proposed squeeze net convolutional neural network provides higher f-measure compared with Mobile net V2 and Res net deep learning model.

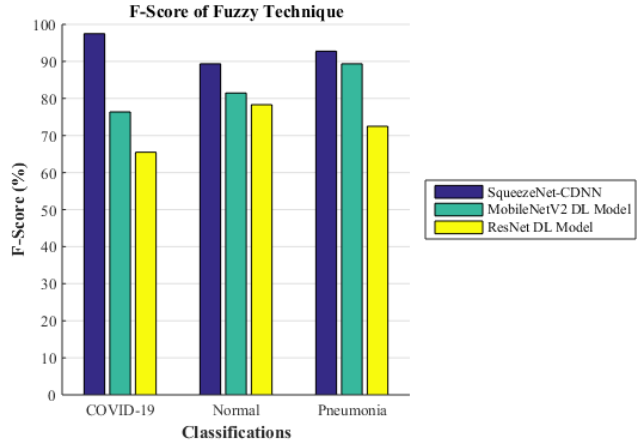

Figure 20: performance analysis of f-score using fuzzy techniques

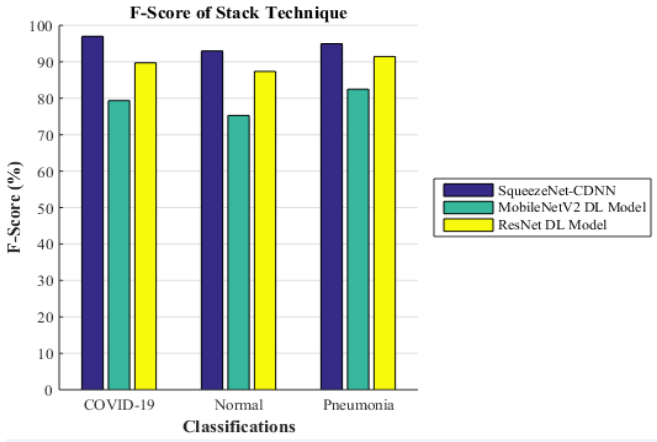

Figure 21: performance analysis of f-score using stacked techniques

6. CONCLUSION

People with COVID-19 can experience permanent damage within lungs that may lead to death. This study aims to differentiate those with lung damage caused by COVID-19 as normal people or pneumonia. COVID-19 diagnosis was administered by deep convolutional neural network models. As it was significant to notice COVID-19 that is spreading quickly and internationally artificial intelligence systems are employed to do this exactly and rapidly. The novel features of the proposed strategy were the use of pre-processing stages of images. While pre-processing steps were used, more effectual characteristics were removed as image data. Through stacking system, every pixel of the equivalent image was overlaid as well as pixels were increased to minimum performance. Based on the proposed strategy, efficient characteristics were removed by the ASA algorithm. This model was designed for providing quicker and accurate outcomes. Another innovative feature was those features packages obtain with ASA were integrated to enhance sorting performance. An overall accuracy of the proposed method produces 97.12 in the squeeze net convolutional neural network model.

REFERENCES

[1] C. Rothe, M. Schunk, P. Sothmann, G. Bretzel, G. Froeschl, C. Wallrauch, T. Zimmer, V. Thiel, C. Janke, W. Guggemos, and M. Seilmaier, **Transmission of 2019-nCoV infection from an asymptomatic contact in Germany.** *New England Journal of Medicine* Vol.382, No. 10, pp. 970-971, 2020.

[2] K. Gostic, A.C. Gomez, R.O. Mummah, A.J. Kucharski, and J.O. Lloyd-Smith. **Estimated effectiveness of symptom and risk screening to prevent the spread of COVID-19.** *Elife*, Vol.9, pp.e55570, 2020.

[3] N. Khan, S. Fahad, M. Naushad, and S. Faisal. **Critical Review of COVID-2019 in the World.** *Available at SSRN 3583925*, 2020.

[4] J. Cohen, **Wuhan seafood market may not be source of novel virus spreading globally**. *Science*, Vol.10, 2020.

[5] Y. Yi, P.N. Lagniton, S. Ye, E. Li, and R.H. Xu, **COVID-19: what has been learned and to be learned about the novel coronavirus disease**. *International journal of biological sciences*, Vol.16, No. 10, pp.1753, 2020.

[6] P.K. Rajagopalan, **The Deadly Corona Virus (Covid-19).** *Journal of Communicable Diseases (E-ISSN: 2581-351X & P-ISSN: 0019-5138)*, Vol. 52, No. 1, pp.78-81, 2020.

[7] R. Keni, A. Alexander, P. Ganesh Nayak, J. Mudgal, and K. Nandakumar. **COVID-19: Emergence, Spread, Possible Treatments, and Global Burden.** *Frontiers in Public Health*, Vol. 8, 2020.

[8] Y. Jin, H. Yang, W. Ji, W. Wu, S. Chen, W. Zhang, and G. Duan. **Virology, epidemiology, pathogenesis, and control of COVID-19.** *Viruses*, Vol. 12, No. 4, pp. 372, 2020.

[9] A.C. Palmenberg, J.A. Rathe, and S.B. Liggett, **Analysis of the complete genome sequences of human rhinovirus**. *Journal of Allergy and Clinical Immunology*, Vol. 125, No. 6, pp.1190-1199, 2010.

[10] J.W. Tang, P. Wilson, N. Shetty, and C.J. Noakes, **Aerosol-transmitted infections—A new**

consideration for public health and infection control teams. *Current Treatment Options in Infectious Diseases*, Vol. 7, No. 3, pp.176-201, 2015.

[11] J. Hamed, Y. Wang, R. Orji, and H. Huang, **Deep sentiment classification and topic discovery on novel coronavirus or covid-19 online discussions: Nlp using lstm recurrent neural network approach**. *arXiv preprint arXiv:2004.11695*, 2020.

[12] R. Sivaramakrishnan, J. Siegelman, P.O. Alderson, L.S. Folio, L.R. Folio, and S.K. Antani. **Iteratively Pruned Deep Learning Ensembles for COVID-19 Detection in Chest X-rays.** *arXiv preprint arXiv:2004.08379*, 2020.

[13] W. Guotai, X. Liu, C. Li, Z. Xu, J. Ruan, H. Zhu, T. Meng, K. Li, N. Huang, and S. Zhang. **A Noise-robust Framework for Automatic Segmentation of COVID-19 Pneumonia Lesions from CT Images**. *IEEE Transactions on Medical Imaging*, 2020.

[14] L. Lin, L. Qin, Z. Xu, Y. Yin, X. Wang, B. Kong, J. Bai, **Artificial intelligence distinguishes COVID-19 from community acquired pneumonia on chest CT.** *Radiology*, pp.200905, 2020.

[15] M. Abdel-Basset, R. Mohamed, M. Elhoseny, R.K. Chakrabortty, and M. Ryan, **A Hybrid COVID-19 Detection Model Using an Improved Marine Predators Algorithm and a Ranking-Based Diversity Reduction Strategy.** *IEEE Access*, Vol. 8, pp.79521-79540, 2020.

[16] D. Das, K.C. Santosh and U. Pal, **Truncated inception net: COVID-19 outbreak screening using chest X-rays**, *Physical and Engineering Sciences in Medicine*, Vol. 43, No. 3, pp. 915-925, 2020.

[17] T. Mahmud, M. Rahman and S. Fattah, **CovXNet: A multi-dilation convolutional neural network for automatic COVID-19 and other pneumonia detection from chest X-ray images with transferable multi-receptive feature optimization**, *Computers in Biology and Medicine*, Vol. 122, pp. 103869, 2020. Available: 10.1016/j.compbiomed.2020.103869

[18] J. Woods, N.T. Hutchinson, S.K. Powers, W.O. Roberts, M.C. Gomez-Cabrera, Z. Radak, I. Berkes, A. Boros, I. Boldogh, C. Leeuwenburgh, and H.J. Coelho-Júnior, **The COVID-19 pandemic and physical activity,** 2020.

[19] D. Kermany, **Identifying Medical Diagnoses and Treatable Diseases by Image-Based Deep Learning**, *Cell*, Vol. 172, No. 5, pp. 1122-1131.e9, 2018. Available: 10.1016/j.cell.2018.02.010

[20] B. Subramani, and M. Veluchamy, **Fuzzy Gray Level Difference Histogram Equalization for Medical Image Enhancement.** *Journal of Medical Systems*. 2020. doi: 10.1007/s10916-020-01568-9

[21] P. Kandhway, A. Bhandari, and A. Singh, **A novel reformed histogram equalization based medical image contrast enhancement using krill herd optimization.** *Biomedical Signal Processing and Control*,Vol.56,pp.101677,2020.doi:10.1016/j.bspc.2019.101677

[22] M. Kaur, and D. Singh, **Fusion of medical images using deep belief networks.** *Cluster Computing*, Vol.23, pp.1439-1453, 2019. doi: 10.1007/s10586-019-02999-x

[23] D. Choi, A. Pazylbekova, W.Zhou, and P. van Beek. **Improved image selection for focus stacking in digital photography**. *In 2017 IEEE International Conference on Image Processing (ICIP)*, pp. 2761-276, 2017.

[24] H. Baloochian, H. Reza Ghaffary, and S. Balochian. **Metaheuristic anopheles search algorithm.** *Evolutionary Intelligence*, pp. 1-13, 2020.

[25] S. Arora, and S. Singh. **Butterfly optimization algorithm: a novel approach for global optimization**. *Soft Computing*, Vol.23, No. 3, pp.715-734, 2019.

[26] Q. Hu, L.F.D.F. Souza, G.B. Holanda, S.S. Alves, F.H.D.S. Silva, T. Han, and PP. Reboucas Filho, **An effective approach for CT lung segmentation using mask region-based convolutional neural networks**. *Artificial Intelligence in Medicine*, Vol.103, pp.101792, 2020.